

Support for anisotropy of the Earth's inner core from free oscillations

Jeroen Tromp

Department of Earth and Planetary Sciences, Harvard University, Cambridge, Massachusetts 02138, USA

IN 1983, Poupinet *et al.*¹ observed that compressional seismic waves traversing the inner core along a trajectory parallel to the Earth's rotation axis arrive faster than the same (PKIKP) waves travelling in the equatorial plane. They interpreted this observation as revealing prolate topography of the inner-core boundary. In 1986, Morelli *et al.*² and Woodhouse *et al.*³ suggested that inner-core anisotropy could explain both the travel-time observations and the anomalous splitting of some of the Earth's normal modes. Inner-core anisotropy continues to be the preferred explanation for the travel-time anomalies, although there is disagreement about the magnitude of anisotropy⁴⁻⁶. More recent explanations for the anomalous splitting involve topography of the inner-core and core-mantle boundaries as well as lateral heterogeneity of the core⁷⁻¹¹. In particular, Widmer *et al.*¹¹ dismissed a rather complex recent model of inner-core anisotropy¹² because it could not explain the splitting of several previously unidentified modes. Here I show that the anomalous splitting of all currently identified modes can in fact be explained by cylindrical anisotropy of the Earth's inner core that is also compatible with the observed PKIKP travel-time anomalies. The resulting model should be regarded as an upper limit to the amount of anisotropy, as lateral heterogeneity also undoubtedly contributes to the splitting.

The evidence for inner-core anisotropy from travel-time data is accumulating but remains inconclusive. Shearer and coworkers^{4,5} proposed uniform anisotropy at the 1% level throughout the inner core, because their PKIKP travel-time observations at distances <155° were smaller than the predictions of the Morelli *et al.*² model. More recently, Creager⁶ showed that there are significant travel-time anomalies between rays turning in the liquid outer core (PKP-BC) and rays turning in the solid inner core (PKIKP) near 150°, contradicting the findings of Shearer *et al.*^{4,5} The model of Creager⁶ requires some 3.5% anisotropy near the top of the inner core, but his data control only the outermost 300 km, and the anisotropy must vanish rapidly below that depth for his model to yield predictions consistent with observations at 180°. The results of Creager⁶ are conceptually compatible with those in Morelli *et al.*² and Woodhouse *et al.*³ The main difference between the analysis of Shearer and coworkers^{4,5} and Creager⁶ is that the former authors used data from the International Seismological Center (ISC), whereas Creager hand-picked PKP-BC minus PKIKP travel-time anomalies. Support for inner-core anisotropy from normal-mode observations appears to be even less conclusive, judging from the incompatible results of Woodhouse *et al.*³, Li *et al.*¹² and Widmer *et al.*¹¹. Because of these discordant claims and results the concept of inner-core anisotropy is in doubt. My aim here is to determine if inner-core anisotropy compatible with the travel-time observations is capable of explaining the splitting observations, or whether another—as yet unknown—cause is required.

A free oscillation or normal mode of the Earth can be characterized by an eigenfunction and an associated eigenfrequency ${}_n\omega_l^m$. The overtone number n angular degree l and azimuthal order m are integers which are used to identify a specific mode of oscillation. For every value of l there are $2l+1$ associated values of m : $m=-l, \dots, m=0, \dots, m=l$. A multiplet ${}_nS_l$ (spheroidal modes) or ${}_nT_l$ (toroidal modes) is the collection of all $2l+1$ free oscillations with the same quantum numbers n and l ; the $2l+1$ members of a multiplet are called singlets. On a

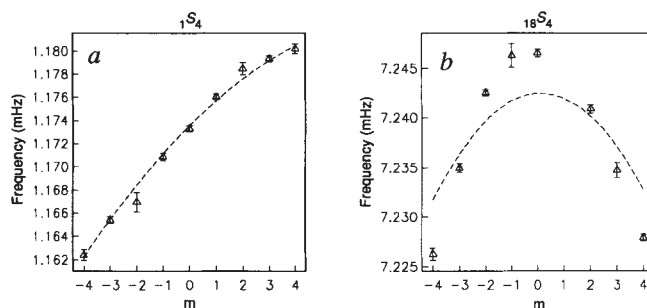


FIG. 1 *a*, Observed and predicted splitting for spheroidal mode ${}_1S_4$. *b*, Observed and predicted splitting for the anomalously split spheroidal mode ${}_{18}S_4$. Observed singlet eigenfrequencies are denoted by triangles. Predicted splitting as a result of the Earth's rotation and ellipticity of figure, equation (1), is indicated by the dashed line.

spherically symmetric Earth model such as PREM¹³, all singlets within a given multiplet have the same eigenfrequency ${}_n\omega_l$; we say that the singlets are $2l+1$ degenerate. Any departure of the Earth from sphericity removes this degeneracy and causes the singlets to split, such that each individual singlet has its own distinct eigenfrequency ${}_n\omega_l^m$.

The Earth's largest deviations from sphericity are its rotation and ellipticity of figure. The associated splitting is predicted to be of the form¹⁴

$$\omega^m = \omega_c(1 + bm + cm^2) \quad (1)$$

where the indices n and l have been omitted for clarity. The parameter ω_c is referred to as the centre frequency of the multi-

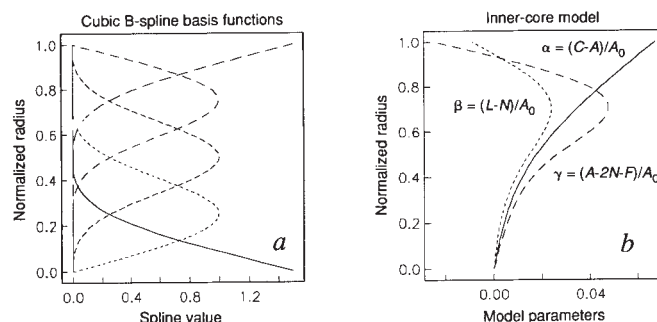


FIG. 2 *a*, Cubic B-spline basis functions used in the inversion¹⁸. A normalized radius of 1 corresponds to the inner-core boundary. The advantage of this representation is that it allows for models that are relatively concentrated in particular regions of the inner core. We are unable to produce a more detailed model of the inner core because of the relatively small data set and because the free oscillations that constitute the data set have only limited radial resolution. The spline functions are used to construct the anisotropic inner-core model. *b*, Anisotropic inner-core model obtained by inversion of the anomalously split modes identified by Ritzwoller *et al.*^{7,9}, Giardini *et al.*¹⁰ and Widmer *et al.*¹². A normalized radius of 1 corresponds to the inner-core boundary. The parameter α shows an overall increase with radius to a maximum value of 6.8% at the inner-core boundary. The parameters β and γ show an overall decrease with radius to minimum values of -0.9 and -2.3% , respectively. The overall behaviour of the parameters α , β and γ with depth is similar to the behaviour of the same parameters in an inner-core model presented by Woodhouse, Giardini and Li³. In that model, based on the seven anomalously split modes ${}_3S_2$, ${}_6S_3$, ${}_9S_3$, ${}_{11}S_4$, ${}_{11}S_5$, ${}_{13}S_2$ and ${}_{13}S_3$, the parameters α , β and γ take on the values 10.4, 1.9 and -3.3% , respectively, at the inner-core boundary and have a prescribed quadratic radial dependence. For a given inner-core model, the centre frequency ω_c is determined separately for each individual multiplet by least-square fitting the observed singlet eigenfrequencies to the predicted singlet eigen frequencies. The 15 spline coefficients are determined by the downhill simplex method²¹ which does not require the calculation of Fréchet derivatives.

plet. The first-order effects of the Earth's rotation are represented by the parameter b and produce linear splitting as a function of m . The Earth's ellipticity of figure and the second-order effects of its rotation are represented by the parameter c and produce quadratic splitting in m . Figure 1a shows an example of the observed and predicted splitting of spheroidal mode ${}_1S_4$ which is predominantly split by rotation.

Masters and Gilbert¹⁵ were the first to identify a collection of modes that is split much more than predicted from the Earth's

rotation and ellipticity of figure. Figure 1b shows an example of an anomalously split mode; this enhanced splitting is characteristic of all such free oscillations. Over the last decade the number of observed anomalously split modes has grown to a total of ~ 20 (refs 3, 7–12). There seems to be general agreement that the structure responsible for the observed splitting is cylindrically symmetric about the Earth's rotation axis and located at or below the core–mantle boundary. Three mechanisms to explain the anomalous splitting have been proposed. The first^{7–11}

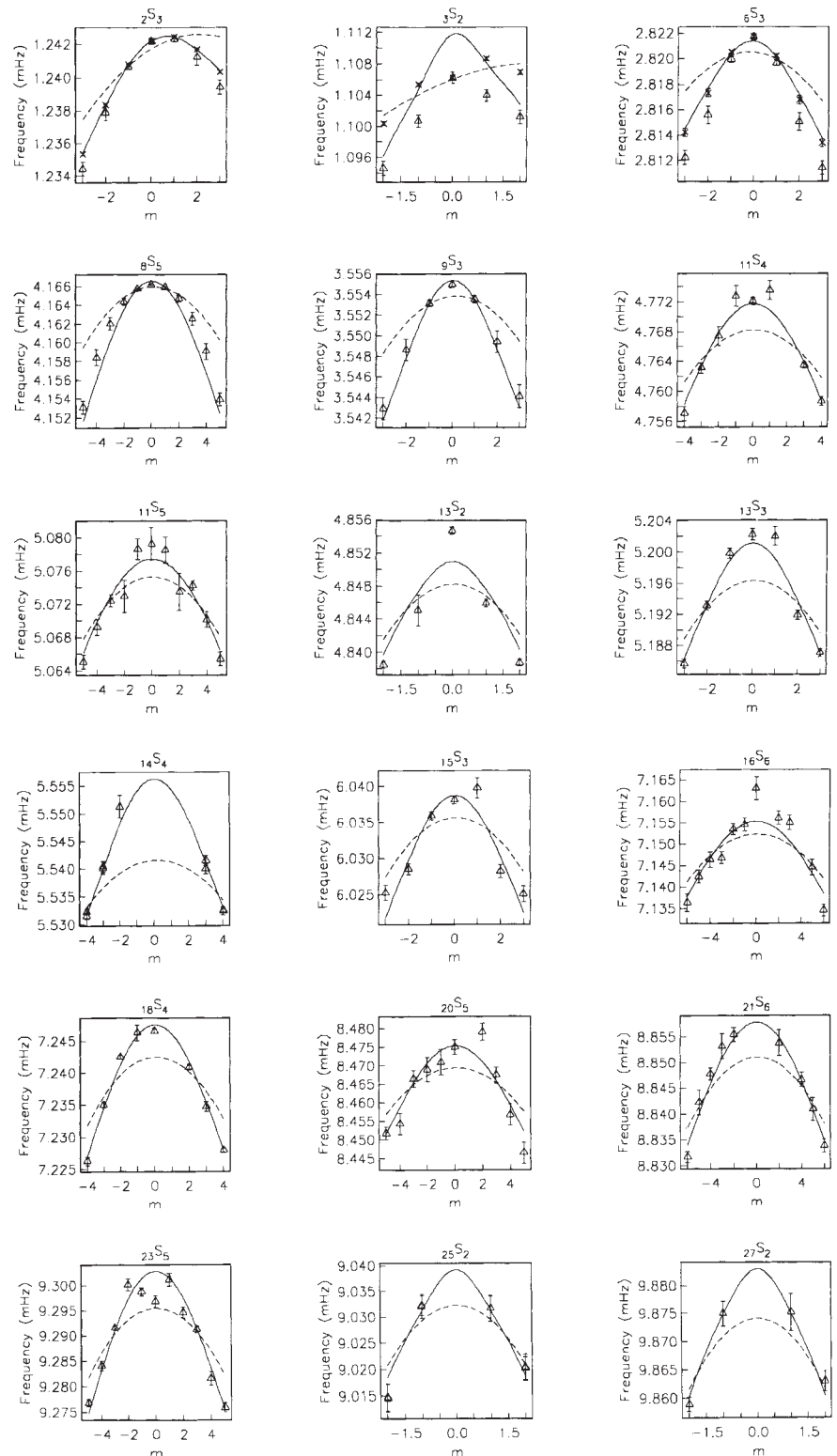
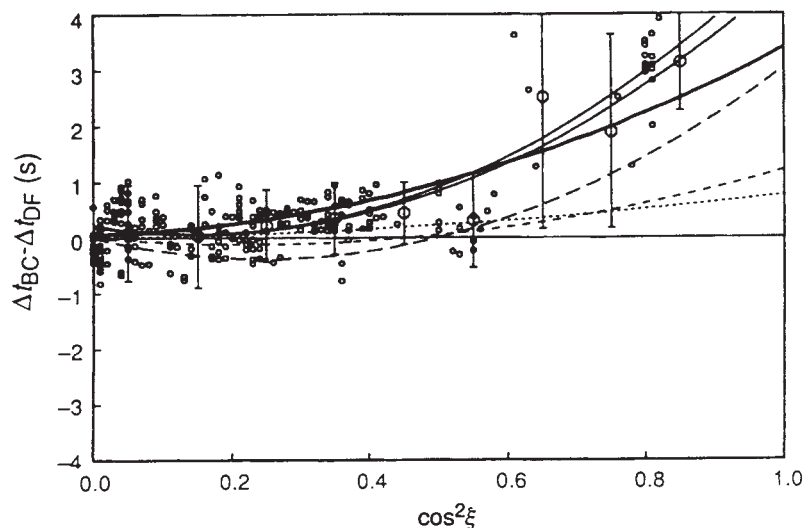


FIG. 3 Observed and predicted splitting for the data set consisting of 18 anomalously split free oscillations. For modes ${}_2S_3$, ${}_3S_2$, ${}_6S_3$, ${}_8S_5$ and ${}_9S_3$, triangles indicate singlet eigenfrequencies obtained from the splitting coefficients published by Ritzwoller *et al.*^{7,9}. For modes ${}_2S_3$, ${}_3S_2$, and ${}_6S_3$, crosses indicate singlet eigenfrequencies obtained from the splitting coefficients published by Giardini *et al.*¹⁰. Finally, for modes ${}_{11}S_4$, ${}_{11}S_5$, ${}_{13}S_2$, ${}_{13}S_3$, ${}_{14}S_4$, ${}_{15}S_3$, ${}_{16}S_6$, ${}_{18}S_4$, ${}_{20}S_5$, ${}_{21}S_6$, ${}_{23}S_5$, ${}_{25}S_2$, and ${}_{27}S_2$, triangles indicate singlet eigenfrequencies determined by Widmer *et al.*¹². Predicted splitting as a result of the Earth's rotation and ellipticity of figure, equation (1), is indicated by the dashed line, and theoretical splitting as a result of rotation, ellipticity, and cylindrical anisotropy of the Earth's inner core, equation (2), is indicated by the solid line. Notice the discrepancy in observed singlet eigenfrequencies for mode ${}_3S_2$, which is one of the few modes that is sensitive to the shear-speed structure of the inner core.

FIG. 4 Predicted and observed PKP-BC minus PKIKP-DF travel-time anomalies due to the anisotropy shown in Fig. 2b plotted as a function of $\cos^2 \xi$, where ξ is the angle between the inner-core leg of the PKIKP ray and the Earth's rotation axis. (This Figure is based upon Fig. 2a of Creager⁶.) The observed anomalies, indicated by the small circles, were determined by Creager⁶. Large circles and bars show mean and two standard deviations of the data binned in 1° intervals. Travel-time anomalies are calculated based upon equation (3) for surface-focus events at an epicentral distance of $\sim 150^\circ$. Thick solid line, this study. The following curves were calculated by Creager⁶: long-dashed line, ref. 2; short-dashed line, ref. 4; dotted line, ref. 5; two thin solid lines, ref. 6.



involves lateral heterogeneity of the core proportional to the spherical harmonic Y_2^0 . Although such models seem to reproduce most of the observed splitting, these studies recognize that the inferred lateral heterogeneity of the core is physically unrealistic¹⁶. The second mechanism involves topography on the inner core and core-mantle boundaries^{1,7,9,10}. With the observed PKIKP travel-time anomalies in mind, the third proposed mechanism^{3,12} involves anisotropy of the inner core that exhibits cylindrical symmetry about the Earth's rotation axis. Topography and lateral heterogeneity seem to be incapable of realistically explaining the PKIKP travel-time observations.

Here I reinvestigate the possibility of a cylindrically anisotropic inner core from the point of view of free oscillations based upon the currently identified anomalously split modes. The simplest type of anisotropy that exhibits cylindrical symmetry about the Earth's rotation axis is transverse isotropy, which involves the five elastic parameters A , C , F , L and N (ref. 17). The parameters C and A correspond to the speed of compressional waves travelling parallel or perpendicular to the Earth's rotation axis, respectively, whereas the parameters L and N correspond to the speed of shear waves travelling parallel or perpendicular to the same axis. The parameter F influences the speed of waves travelling at other angles with the rotation axis. It can be demonstrated (J.T., manuscript in preparation) that this type of anisotropy together with rotation and ellipticity produces splitting of the form

$$\omega^m = \omega_c'(1 + bm + cm^2 + c'm^2 + dm^4) \quad (2)$$

The coefficients c' and d represent the effects of inner-core anisotropy and are completely determined by the three parameters $\alpha = (C - A)/A_0$, $\beta = (L - N)/A_0$, and $\gamma = (A - 2N - F)/A_0$, where $A_0 = \kappa + \frac{4}{3}\mu$ is determined by the bulk modulus κ and shear modulus μ at the centre of the reference Earth model. When $\alpha > 0$, inner-core P waves travel slower in the equatorial plane than along the Earth's rotation axis. Similarly, when $\beta > 0$, inner-core S waves travel slower in the equatorial plane than along the Earth's rotation axis; such inner-core S waves have never been unambiguously observed. The third parameter, γ , influences the speed of P and S waves travelling in directions other than parallel or perpendicular to the axis of rotation. Using a data set collected by Ritzwoller *et al.*^{7,9}, Giardini *et al.*¹⁰ and Widmer *et al.*¹¹ consisting of the 18 anomalously split multiplets $2S_3$, $3S_2$, $6S_3$, $8S_5$, $9S_3$, $11S_4$, $11S_5$, $13S_2$, $13S_3$, $14S_4$, $15S_3$, $16S_6$, $18S_4$, $20S_5$, $21S_6$, $23S_5$, $25S_2$ and $27S_2$, for a total of 145 singlet eigenfrequencies, I invert for the radial dependence of α , β and γ .

I represent the radial dependence of the three model parameters α , β and γ in terms of five cubic B-spline basis

functions¹⁸, as shown in Fig. 2a. I seek to determine five spline coefficients for each of the three model parameters, which makes for a total of 15 unknowns. Figure 2b shows the resulting inner-core model. The splitting predicted for the 18 anomalously split modes in the data set is shown in Fig. 3. The reduction in variance achieved by the model in Fig. 2b compared to a model incorporating only the effects of rotation and ellipticity is 72%. The value of χ^2/ν , where $\nu = 145 - 15 = 130$ is the number of degrees of freedom, is 17.0 for the initial model based upon rotation and ellipticity and 3.4 for the final model based upon rotation, ellipticity and inner-core anisotropy. The details of the top of the inner-core model in Fig. 2b were based on recent travel-time observations (W.-J. Su and A. Dziewonski, manuscript in preparation), particularly in the epicentral distance range 130 – 136° . It is interesting to note that modes such as $11S_4$, $11S_5$ and $16S_6$, which have $<2\%$ of their energy in the inner core, are nevertheless reasonably well fitted by the model. (Widmer *et al.*¹¹ used the relatively small percentage of inner-core energy of some anomalously split modes as an argument against inner-core anisotropy.) Note, also, that the inner-core model of Woodhouse *et al.*³, which is compatible with the model in Fig. 2b, produces the observed splitting with a variance reduction of 56%. An anisotropic inner-core model proposed by Creager⁶, which was designed to fit travel-time anomalies, can also produce the observed splitting, with a similar variance reduction, provided I restrict Creager's uniform anisotropy to the upper 300 km of the inner core.

The P velocity (v) perturbation associated with the model shown in Fig. 2b is given by²

$$\frac{\delta v}{v} = (2\beta - \gamma) \cos^2 \xi + (\frac{1}{2}\alpha - 2\beta + \gamma)(\cos^2 \xi)^2 \quad (3)$$

where ξ is the angle between the PKIKP ray segment in the inner core, and the Earth's rotation axis. Although travel-time observations are not included in the inversion, I do force it to look for models that are compatible with those observations; this procedure does not significantly affect the fit to the normal-mode data. In Fig. 4 the travel-time anomaly between rays turning in the outer core (PKP-BC) and those turning in the inner core (PKIKP) due to the anisotropy shown in Fig. 2b is plotted as a function of $\cos^2 \xi$. The predicted travel-time anomalies agree quite well with the observed anomalies of Creager⁶. PKIKP travel times of waves travelling parallel to the Earth's rotation axis are 2.6 s faster than for waves travelling in the equatorial plane, which is also on the order of the observed PKIKP travelling time anomalies².

To decide the issue of inner-core anisotropy based upon travel times probably requires taking a new look at the records used

by the ISC. If we are willing to accept the hypothesis that the inner core exhibits cylindrical anisotropy, this raises the question of what physical process could be responsible for this phenomenon. Previous studies^{19,20} suggest that the inner core consists of iron in its hexagonally close-packed phase; this ε -phase of iron has cylindrical symmetry, which would be in agreement with the results described here. □

Received 20 May; accepted 19 October 1993.

1. Poupinet, G., Pillet, R. & Souriau, A. *Nature* **305**, 204–206 (1983).
2. Morelli, A., Dziewonski, A. M. & Woodhouse, J. H. *Geophys. Res. Lett.* **13**, 1545–1548 (1986).
3. Woodhouse, J. H., Giardini, D. & Li, X.-D. *Geophys. Res. Lett.* **13**, 1549–1552 (1986).
4. Shearer, P. M. & Toy, K. M. & Orcutt, J. A. *Nature* **333**, 228–232 (1988).
5. Shearer, P. M. & Toy, K. M. *J. Geophys. Res.* **96**, 2233–2247 (1991).
6. Creager, K. C. *Nature* **356**, 309–314 (1992).
7. Ritzwoller, M., Masters, G. & Gilbert, F. *J. Geophys. Res.* **91**, 10203–10228 (1986).
8. Giardini, D., Li, X.-D. & Woodhouse, J. H. *Nature* **325**, 405–411 (1987).

9. Ritzwoller, M., Masters, G. & Gilbert, F. *J. Geophys. Res.* **93**, 6369–6396 (1988).
10. Giardini, D., Li, X.-D. & Woodhouse, J. H. *J. Geophys. Res.* **93**, 13716–13742 (1988).
11. Widmer, R., Masters, G. & Gilbert, F. *Geophys. J. Int.* **111**, 559–576 (1992).
12. Li, X.-D., Giardini, D. & Woodhouse, J. H. *J. Geophys. Res.* **96**, 551–557 (1991).
13. Dziewonski, A. M. & Anderson, D. L. *Phys. Earth planet. Inter.* **25**, 297–356 (1981).
14. Woodhouse, J. H. & Dahlen, F. A. *Geophys. J. R. astr. Soc.* **53**, 335–354 (1978).
15. Masters, G. & Gilbert, F. *Geophys. Res. Lett.* **8**, 569–571 (1981).
16. Stevenson, D. *Geophys. J. R. astr. Soc.* **68**, 311–319 (1987).
17. Love, A. E. H. *A Treatise on the Mathematical Theory of Elasticity* 4th edn (Cambridge Univ. Press, 1927).
18. Michelini, A. & McEvilly, T. V. *Bull. seism. Soc. Am.* **81**, 524–552 (1991).
19. Brown, J. M. & McQueen, R. G. *J. Geophys. Res.* **91**, 7485–7494 (1986).
20. Anderson, O. L. *Geophys. J. R. astr. Soc.* **84**, 561–579 (1986).
21. Press, W. H., Flannery, B. P., Teukolsky, S. A. & Vetterling, W. T. *Numerical Recipes in C* (Cambridge Univ. Press, 1988).

ACKNOWLEDGEMENTS. I thank R. Widmer for his data set of observed singlet eigenfrequencies and for suggestions regarding those data; K. Creager for his data set of observed travel-time anomalies; W.-J. Su and A. Dziewonski for the opportunity to fit their new data set of PKP-BC minus PKIKP travel-time anomalies; G. Ekström for software for the calculation of cubic B-splines; and A. Dziewonski, G. Ekström, J. Woodhouse, M. Ritzwoller, G. Masters and W.-J. Su for discussions and suggestions. This research was supported by the US National Science Foundation.

Rapid human-induced evolution of insect–host associations

Michael C. Singer*, Chris D. Thomas† & Camille Parmesan*

* Department of Zoology, University of Texas, Austin, Texas 78712, USA

† School of Biological Sciences, University of Birmingham, Edgbaston B15 2TT, UK

RAPID evolution of host association is now occurring independently in two populations of the host-specialist butterfly *Euphydryas editha*, each of which has recently incorporated a novel host species into its diet. The reasons for these episodes of rapid evolution lie in human land use practices: logging in one case and cattle ranching in the other. In contrast to other insects that have used tolerance of human activities to expand their ranges into disturbed habitats^{1–3}, these rare butterflies have remained at their original sites and evolved adaptations to the changes occurring at those sites. At both sites, the proportion of insects preferring the novel host has increased, in one case clearly because of genetic changes in the insect population. This process is now starting to generate insects that refuse to accept their ancestral host, foreshadowing a new problem in conservation biology. By adapting genetically to human-induced changes in their habitat, the insects risk becoming dependent on continuation of the same practices. This is a serious risk, because human cultural evolution can be even faster than the rapid genetic adaptation that the insects can evidently achieve.

Our study insect, *Euphydryas editha*, belongs to a group of Nymphalid butterflies known in the UK as fritillaries (related to the marsh fritillary) and in the USA as checkerspots. One of the few (<6) known populations of *E. editha monoensis*, which is currently on the list of candidates for endangered status, lives at our Schneider study site (Ormsby Co., Nevada). Evidence for recent diet change by the insects at this site is their use of the European weed, *Plantago lanceolata*, introduced by cattle ranchers⁴. Comparison with nearby *E. editha* populations where *P. lanceolata* has not been introduced suggests that the ancestral diet of Schneider butterflies was *Collinsia parviflora*⁴. Although *C. parviflora* has recently supported much lower larval survival than *P. lanceolata*⁵, the Schneider butterflies still use both host species. A third host, *Penstemon rydbergii*, normally receives few eggs.

In nearby sites where *P. lanceolata* has not been introduced, we found no butterflies that preferred it, but about 10% of them accepted it as readily as *C. parviflora*⁴. At Schneider, we did find insects that actively preferred the introduced host, *P. lanceolata*⁴.

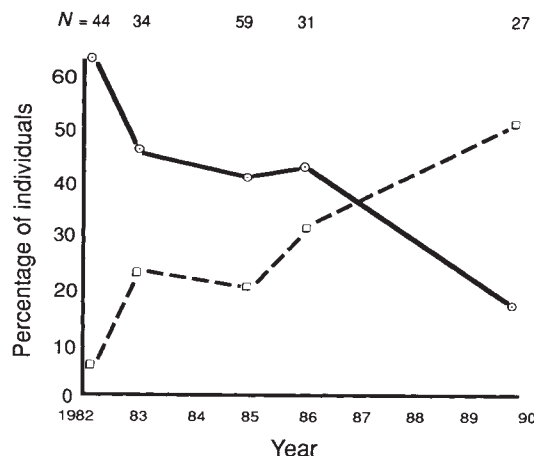


FIG. 1 Changes over time in results of preference trials done in the field at Schneider's Meadow. Each trial was conducted with contemporary plants, undisturbed and still growing in their natural positions. Each insect was repeatedly offered two hosts in alternation, but not allowed to oviposit. Such insects usually pass through three phases: a rejection phase when neither host is accepted, a discrimination phase when one host is consistently accepted and the other consistently rejected, and a final phase when both are accepted until oviposition is allowed by the experimenter²³. The preferred host is the one that is accepted during the discrimination phase. Data are given for proportions of insects preferring each of the two hosts. The proportion of insects without preference is not presented explicitly, but can be deduced from the figure, because the three categories sum to 1. The ratio of the number of insects preferring *P. lanceolata* (□) to the number preferring *C. parviflora* (○) is significantly heterogeneous among years. (Contingency table analysis, $G = 27.7$, d.f. = 3, $P = 0.0001$.)

The proportion of these insects in the population has risen sharply in the past decade (Fig. 1), as has the proportion actually using *P. lanceolata* (Table 1). To determine whether genetic change in insect preference had occurred, we compared the preferences of greenhouse-reared offspring of butterflies captured in 1983 and 1990. These preferences differed in the same direction as the change measured in the field (Table 2). This result provides strong evidence for genetic change of preference in the insect population over the seven generations from 1983 to 1990. This is a direct demonstration of the evolution of an insect–plant association. Previously, such changes in non-pest systems were inferred from contemporary patterns, not observed directly^{6–16}. One other natural episode of rapid diet-associated evolution has been observed: the bill width of a seed-eating bird, *Geospiza fortis*, decreased following a change in the available diet¹⁷.

Several factors predispose Schneider *E. editha* to rapid diet